Loop-Current Fluctuations Mediated Chiral *d*-Wave Pairing in Kagome Lattice

Qi-Fang Li[1,2], Gaopei Pan[3], Xu Zhang[4], Satoru Nakatsuji[1,5], Weilun Jiang[6,7*], Xiao Yan Xu[8,9*], and Xianxin Wu[2*]

[1]*Institute for Solid State Physics, University of Tokyo, Kashiwa, Chiba, 277-8581, Japan*
[2]*CAS Key Laboratory of Theoretical Physics, Institute of Theoretical Physics, Chinese Academy of Sciences, Beijing 100190, China*
[3]*Institut für Theoretische Physik und Astrophysik and Würzburg-Dresden Cluster of Excellence ct.qmat, Universität Würzburg, 97074 Würzburg, Germany*
[4]*Department of Physics and Astronomy, University of Ghent, Ghent, 9000, Belgium*
[5]*Department of Physics, University of Tokyo, Hongo, Bunkyo-ku, Tokyo, 113-0033, Japan*
[6]*Institute of Opto-Electronics, Shanxi University, Taiyuan 030006, China*
[7]*Collaborative Innovation Center of Extreme Optics, Shanxi University, Taiyuan 030006, China*
[8]*Key Laboratory of Artificial Structures and Quantum Control (Ministry of Education), School of Physics and Astronomy, Shanghai Jiao Tong University, Shanghai 200240, China*
[9]*Hefei National Laboratory, Hefei 230088, China*

(Received 13 March 2025; accepted manuscript online 15 April 2025)

Recent various experiments have provided evidence supporting the emergence of loop-current order in kagome metals. Particularly superconductivity in AV_3Sb_5 is significantly enhanced when this charge order is suppressed by pressure or doping. Distinct from magnetic order, loop-current order does not couple directly to spin and thus whether such fluctuations can enhance superconductivity remains elusive. We design a sign problem-free bilayer kagome model coupled to quantum Ising spins through bond currents and perform determinant quantum Monte Carlo simulations to explore single-particle properties and superconductivity arising from 2×2 loop-current fluctuations. We find that this loop-current order induces intriguing band folding, band broadening, and gap opening around saddle points. Remarkably, our pairing susceptibility analysis identifies a dominant enhancement of superconductivity due to loop-current fluctuations, with the dominant pairing being the chiral *d*-wave channel. This pairing primarily occurs within the intra-sublattice channel and involves third nearest-neighbor sites, attributed to the unique sublattice texture associated with van Hove singularities. We also discuss potential experimental implications for kagome superconductors.

DOI: 10.1088/0256-307X/42/5/057302 CSTR: 32039.14.0256-307X.42.5.057302

1. Introduction. Recently, kagome metals such as AV_3Sb_5 (A = K, Rb, Cs)[1–4] and FeGe,[5–8] which feature van Hove singularities (VHSs) near the Fermi level, have garnered significant attention due to their emergent and diverse quantum orders, including superconductivity, charge density wave (CDW), and nematicity. Unlike the intriguing magnetic properties of traditional kagome materials, these kagome metals host CDW order with exotic properties intimately linked to VHSs. In both AV_3Sb_5 and FeGe, a CDW transition occurs below T_{CDW} and exhibits an in-plane 2×2 configuration. Intriguingly, muon spin resonance (μSR), magneto-optical Kerr effect, and chiral transport measurements in AV_3Sb_5 have provided evidence of time-reversal symmetry (TRS) breaking within the CDW phase in the absence of magnetic ordering.[9–13] In the antiferromagnet FeGe, an enhancement of the magnetic moment and anomalous Hall effect have been observed upon the CDW transition.[7,14] These experimental findings suggest the occurrence of loop-current order (LCO) within the kagome lattice.[15–18] In AV_3Sb_5, superconductivity subsequently emerges within the CDW phase, and double superconducting domes have been observed under pressure.[19] Remarkably, a tripling of T_c is achieved when the CDW is suppressed by pressure, indicating a close relationship between superconductivity and CDW fluctuations.

In cuprates, the TRS-breaking LCO has been proposed as a hidden order in the pseudogap phase, with its fluctuations potentially generating marginal Fermi liquid behavior and *d*-wave superconductivity near the quantum-critical point (QCP).[20,21] Typically, when a QCP is approached, the associated fluctuations significantly enhance superconductivity in certain channels;[22–24] for instance, antiferromagnetic fluctuations promote spin-singlet pairing. Unlike magnetic orders with local moments, LCO exhibits orbital magnetism and does not directly couple to spin. Recent studies have shown an absence of enhanced superconductivity near QCP of intra-unit cell LCO on the square lattice.[25] In the context of the kagome lattice near

*Corresponding author. Email: wljiang@sxu.edu.cn; xiaoyanxu@sjtu.edu.cn; xxwu@itp.ac.cn
© 2025 Chinese Physical Society and IOP Publishing Ltd. All rights, including for text and data mining, AI training, and similar technologies, are reserved.

van Hove filling, the relevant LCO is 2×2, featuring a complex current pattern as suggested by experimental and theoretical studies.[15–18,26] Whether such an LCO can enhance superconductivity and which type of pairing may be favored remain elusive. Additionally, the unique sublattice texture associated with VHSs in the kagome lattice plays a critical role in determining correlated states,[27–32] and its interaction with loop-current fluctuations is yet to be explored. To address these issues, it is essential to construct a model capturing all relevant features and treat all fluctuations in an unbiased manner.

Motivated by these fundamental questions, we have designed a fermionic bilayer kagome model coupled to quantum Ising spins via bond currents, incorporating quantum fluctuations of loop-current order. This model is sign problem-free, allowing us to perform numerical determinant quantum Monte Carlo (DQMC)[33–35] calculations to investigate the single-particle properties and superconductivity arising from these quantum fluctuations near the QCP. We find that the 2×2 LCO induces interesting band folding and gap opening around VHSs. Remarkably, we identify a significant enhancement of chiral d-wave pairing near the QCP due to the loop-current fluctuations. This pairing predominantly occurs in the intra-sublattice channel and involves the third nearest-neighbor sites because of the unique sublattice texture associated with VHSs. We also discuss the experimental implications of our results for kagome superconductors.

2. Theoretical Model. We consider a two-dimensional model of itinerant fermions on a kagome lattice coupled to an Ising ferromagnet on a honeycomb lattice with a transverse field [Fig. 1(a)]. The Hamiltonian consists of three parts: fermions, bosons, and boson–fermion couplings:

$$\hat{H} = \hat{H}_{\rm f} + \hat{H}_{\rm b} + \hat{H}_{\rm f-b}. \tag{1}$$

The fermion part of the Hamiltonian $\hat{H}_{\rm f}$ describes spin-1/2 fermions on a 2D kagome lattice with nearest-neighbor hopping and two orbitals. This Hamilton reads

$$\hat{H}_{\rm f} = -t\sum_{\langle i,j\rangle}\sum_{\sigma,\lambda}(\hat{c}^{\dagger}_{i\sigma\lambda}\hat{c}_{j\sigma\lambda} + {\rm h.c.}) - \mu\sum_{\langle i,j\rangle}\sum_{\sigma,\lambda}\hat{n}_{i\sigma\lambda}, \tag{2}$$

where t is the hopping, $\sigma = \uparrow,\downarrow$ labels the spin, and the orbit index $\lambda = \pm$ denotes the upper/lower layers shown in Fig. 1(a). μ is the chemical potential and determines the fermion density in the grand canonical ensemble.

The bosonic part $\hat{H}_{\rm b}$ corresponds to a transverse Ising model and reads

$$\hat{H}_{\rm b} = -J\sum_{\langle p,q\rangle}\hat{S}^z_p\hat{S}^z_q - h\sum_p \hat{S}^x_p, \tag{3}$$

where J is the ferromagnetic coupling and h is the transverse field in the x-direction, perpendicular to the Ising spins along the z-direction. The bosonic Ising spins $\{S_p = \pm1\}$ amid with two orbitals of kagome lattices are located at the centers of the triangles in the 2D kagome lattice, forming a honeycomb lattice. By tuning the competition between quantum fluctuation and the ferromagnetic order, the transverse field h in x-direction plays a crucial role in driving the system through a quantum phase transition.

The boson–fermion coupling term represents interactions between the Ising spins and charge bond currents within the smallest triangles of both orbitals surrounding the Ising spin in the xy-plane,

$$\hat{H}_{\rm f-b} = \xi\sum_{\substack{i\to j\\ \langle p,i,j\rangle}}\sum_{\sigma,\lambda}\lambda[({\rm i}\epsilon_{ij}\hat{c}^{\dagger}_{j\sigma\lambda}\hat{c}_{i\sigma\lambda} + {\rm h.c.})\hat{S}^z_p]. \tag{4}$$

Here, ξ is the boson–fermion coupling constant and ϵ_{ij} is a permutation variable that takes the value 1 if $i\to j$ follows the direction of the loop current and -1 otherwise. The loop current configuration within each kagome layer is 2×2 and preserves the six-fold rotational symmetry, as suggested from theoretical prior studies.[15] The current patterns between two layers are connected by the time-reversal symmetry. Our model preserves an effective anti-unitary symmetry $\mathcal{T} = -{\rm i}\tau_y\mathcal{K}$, with τ_y in the layer space and $\mathcal{K}$ being the complex conjugation operation. This symmetry ensures that our model is sign problem-free,[36] allowing for a numerically exact simulation based on DQMC. The details of our DQMC calculations[37] are provided in the supplementary materials (SM) and we conduct calculations with varying system size, from $L = 6$ to 12, and down to the lowest temperature of $T = 0.05t$ ($\beta t = 20$).

3. Phase Diagram. In the absence of boson–fermion coupling $\xi = 0$, the transverse-field Ising model on the honeycomb lattice shows a typical ferromagnetic–paramagnetic (FM–PM) phase transition. The phase boundary is shown as blue dots in Fig. 1(b), based on our

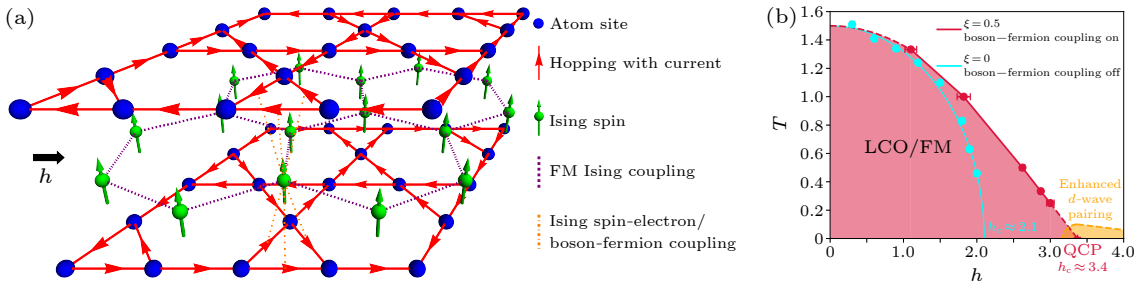

Fig. 1. (a) Sketch of model defined in Eq. (1). Two layers (orbitals) of a kagome lattice with 2×2 chiral electric current are coupled to honeycomb Ising fields situated between the layers. (b) A phase diagram of the LCO, along with a rough illustration of the region with enhanced d-wave pairing near the quantum critical points.

numerical calculations. We extrapolate the quantum phase transition point at zero temperature to be $h_c = 2.1$ using finite-size scaling crossing analysis, which is consistent with the value 2.13 reported in previous numerical work.[38] The FM–PM transition at zero temperature without coupling belongs to the (2+1)D Ising universality class.

By switching on the coupling between fermions and Ising spins, we further study the itinerant FM–PM transition. Throughout this work, unless otherwise specified, we use a representative coupling constant $\xi = 0.5$ and a chemical potential $\mu = 0.5$. We set $t = J = 1$ as the energy unit. The chemical potential is chosen to slightly deviate from the upper van Hove singularity, where the density of states (DOS) is divergent. Tuning on this coupling shifts the phase boundary [red dots and line in Fig. 1(b)] to higher temperature and transverse field. This indicates that the effective ferromagnetic coupling is enhanced when integrating out the fermions. At finite temperature, the FM–PM phase transition belongs to 2D Ising universality class, as the fermions are gapped and can be trivially integrated out. At zero temperature, the coupling between the gapless fermions and the critical bosons may drive a new itinerant QCP or a first order transition. Since our simulations cannot access the zero-temperature limit, this remains an open question. However, if there is a QCP at zero temperature, we can perform a linear extrapolation to obtain a rough estimate of its position, which is $h_c = 3.4$.

Specifically, in the FM phase, the Ising spin has a finite magnetization $\langle \hat{S}_p^z \rangle = M \neq 0$. On the mean field level, $\hat{H}_{f-b}$ is just the Hamiltonian of the 2×2 LCO for fermions on the kagome lattice.[15] Thus, the presence of FM order in the Ising model corresponds to the occurrence of 2×2 LCO for fermions on the kagome lattice, while a PM phase indicates its absence. Near QCP, the quantum fluctuations associated with Ising spin introduce loop-current fluctuations with wave vectors of $\boldsymbol{Q}_M$ for fermions, where non-Fermi liquid behavior and unconventional pairing may appear. In the following, we focus on the impact on electronic structure and unconventional pairing stemming from loop-current fluctuations [as shown in Fig. 1(b)]. We find a strong pairing tendency in the chiral d-wave channel near QCP by the analysis of pairing susceptibilities.

4. Impact of Loop-Current Fluctuations on Electronic Structure. In the FM phase, the order parameter of 2×2 LCO can be replaced by $\xi_{\text{eff}} = M\xi$ at the mean-field level. The corresponding unfolded band structure[39] (red curves) is shown in Fig. 3(a) with $\xi_{\text{eff}} = 0.5$, compared with the kagome band structure. We observe that this LCO introduce significant band folding and large gap opening, especially around both upper and lower VHSs around M points. Additionally, flat bands are split and Dirac cones are gapped. The fermionic system is insulating at $\mu = 0.5$. To include effect of quantum fluctuations, we perform DQMC calculations for the whole model and obtain spectral functions $A(\boldsymbol{k}, \omega)$ at different h values by using stochastic analytical continuation method[40–43] for the imaginary-time Green's function. We select three representative cases: $h = 4.0$ for paramagnetic Ising spins without LCO, $h = 3.4$ around the QCP with significant quantum fluctuations, and $h = 1.0$ for ferromagnetic Ising spins with LCO. At a high transverse field $h = 4.0$, the sharp spectral function near the Fermi level overlaps with kagome bands. Around the QCP, the fluctuations broaden the spectral function and the weak LCO introduces clear band folding and small gap opening around VHSs, as shown in Fig. 2(c). The fermionic systems stay metallic and the upper van Hove point is split into three states, with two high-energy states showing higher spectral intensity. Within the FM phase, the LCO is fully established.

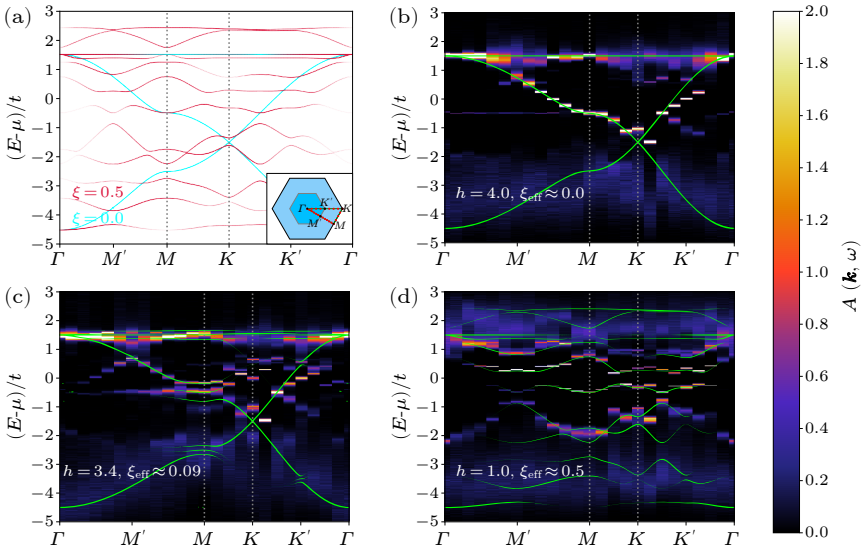

Fig. 2. Unfolded spectral functions and mean-field band structures for different transversed fields h. (a) Comparison of the unfolded band structure of kagome lattice with (red curves) and without LCO (blue curvers). (b) Spectral function for a strong external field with absence of LCO. (c) Spectral function near the QCP. (d) Spectral function for a weak external field with a full 2×2 LCO. Original three bands split throughout Brillouin zone, except at Γ, and an energy gap appears near Fermi surface. The mean-field unfold band dispersions are blue with corresponding order parameter ξ_{eff} indicated in the plots.

Consequently, as shown in Fig. 2(d), the gap opening around the Fermi level reaches its maximum and the flat band becomes smeared, resulting in an insulating phase.

Furthermore, we study the evolution of the Fermi surface characteristics as a function of the transverse field. In the single-particle kagome model, the upper van Hove singularity exhibits a unique sublattice texture, where the wavefunction at each saddle point is solely attributed to one sublattice.[44] As the adopted Fermi level is slightly away from van Hove filling, the sublattice texture on Fermi surface is inherited, as shown in Fig. 3(a). The Fermi points close to the M points carry large DOS and have pure-sublattice contribution. With including boson–fermion coupling, the spectral weight at the Fermi level can be obtained from the Green's function $G(\boldsymbol{k}, \beta/2)$ by using the relation $G(\boldsymbol{k}, \tau) = \int \mathrm{d}\omega \frac{\mathrm{e}^{-\omega(\tau-\beta/2)}}{2\cosh(\beta\omega/2)} A(\boldsymbol{k}, \omega)$.[45] With $T = 0.05$, figures 3(b)–3(d) plot the Fermi surfaces for various transverse fields h across the QCP of LCO. In the strong h limit paramagnetic state, the Fermi surface resembles to the non-interacting case except for some thermal broadening, as shown in Fig. 3(b). Near the QCP, as indicated from Fig. 3(c), the gap at points close to M fills in and this leads to broadening spectral function, compared with other points. In the ordered state, the 2×2 LCO gaps out the whole Fermi surface and generate an insulating phase, as shown in Fig. 3(d).

5. Enhanced Chiral d-Wave Pairing Near QCP. Now we explore the superconductivity near the QCP of LCO, where the loop-current fluctuations are pronounced. Unlike magnetic order, LCO does not directly couple to spin, leaving it unclear whether such quantum fluctuations can enhance superconductivity. We consider uniform superconducting pairing in both intralayer and interlayer channels and calculate the corresponding susceptibilities. In the intralayer pairing channel, the spin-singlet/spin-triplet pairing terms can be written as

$$\Delta_{1\alpha l}^{S/T} = \sum_{i,\lambda,\delta_l \in \{l\}} f_{i\delta_l}^{\alpha} [\hat{c}_{i\uparrow\lambda}\hat{c}_{(i+\delta_l)\downarrow\lambda} \mp \hat{c}_{i\downarrow\lambda}\hat{c}_{(i+\delta_l)\uparrow\lambda}]. \quad (5)$$

Here $f_{i\delta_l}^{\alpha}$ is the normalized pairing form factor between i and $i+\delta_l$ site in the $\alpha = s, p, d$ channel and δ_l is the vector connecting l-th nearest-neighbor (n.n.) sites, as indicated in Fig. 4(a). We consider pairing up to the third n.n. and there are two types of third n.n. pairing: 3rd diagonal n.n. and 3rd stripe n.n., as shown in Fig. 4(a). For the interlayer channel, we consider two pairing terms,

$$\Delta_{2s0}^{S/T} = \frac{1}{\sqrt{2}} \sum_i (\hat{c}_{i\uparrow+}\hat{c}_{i\downarrow-} \mp \hat{c}_{i\downarrow+}\hat{c}_{i\uparrow-}). \quad (6)$$

The other interlayer pairings are neglected as we focus on the intralayer pairing from quantum fluctuations. To study the pairing tendency in different channels, we calculate pairing susceptibilities defined as

$$\chi_{\eta}^{S/T} = \int_0^{\beta} \mathrm{d}\tau \langle [\Delta_{\eta}^{S/T}(\tau)]^{\dagger} \Delta_{\eta}^{S/T}(0) \rangle, \quad (7)$$

with $\eta = m\alpha l$. They can be evaluated within our DQMC calculations for various transverse fields and temperatures, with details provided in SM.

We have performed calculations with different system sizes and they exhibit similar qualitative behaviors. Here, we present data of $L = 10$ as a representative example. Figure 4(b) shows the susceptibility of interlayer pairing as a function of transverse field for different inverse temperatures. At high temperature, with increasing h, the susceptibility initially rises rapidly, reaches the maximum at h_c then gradually decreases. When $T < 1/12$, the susceptibility increases sharply around h_c and quickly decreases for $h > h_c$, showing a sharp peak around h_c. In addition, the susceptibility at h_c increases with decreasing temperature. These behaviors indicate onsite quantum fluctuations enhance interlayer pairing, consistent with findings from other bilayer models.[46] However, the interlayer pairing is not associated with fluctuations of the 2×2 LCO of interest, which primarily induces intralayer pairing.

In the intralayer channel, we find that quantum-fluctuations can indeed enhance superconductivity near QCP, with the corresponding pairing mainly occurring in the intra-sublattice channel (onsite, third n.n.) not inter-sublattice channel (n.n. and second n.n). This effect is intimately related to the sublattice texture on the Fermi surface, shown in Fig. 3(a). The $\pm\boldsymbol{k}$ points involved in pairing mainly show pure-sublattice nature in regions of high DOS (near M points). Figure 4(c) displays the susceptibilities for the third stripe n.n. d-wave. The main features are similar to those observed in interlayer pairing, however, one notable difference is that the susceptibility shows a slower decrease when h exceeds h_c and is almost flat. This behavior is consistent with spin-density-wave fluctuation induced d-wave pairing in the square lattice.[47] To identify the dominant pairing, we plot the susceptibilities in different channels at $T = 0.05$ in Fig. 4(d). It is apparent that the third stripe n.n. d-wave pairing exhibits the largest susceptibility and strongest enhancement near QCP, compared with other s- and p-wave pairing. Figure 4(e) shows susceptibilities at $h_c = 3.4$ as a function of temperature, where they show a continuous increase with decreasing T. However, we do not observe a divergence of susceptibility for the d-wave pairing down to $T = 0.05$,

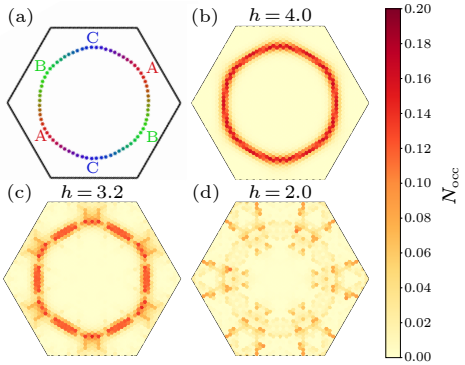

Fig. 3. Shape of the Fermi surface. (a) Contributions coded by colors of sublattices at the Fermi surface. (b) For large h, LCO is absent and the gap remains closed. (c) Near the critical field h_c, LCO induces a topological change in the band structure. (d) For small h, LCO dominates, leading to a fully gapped Fermi surface.

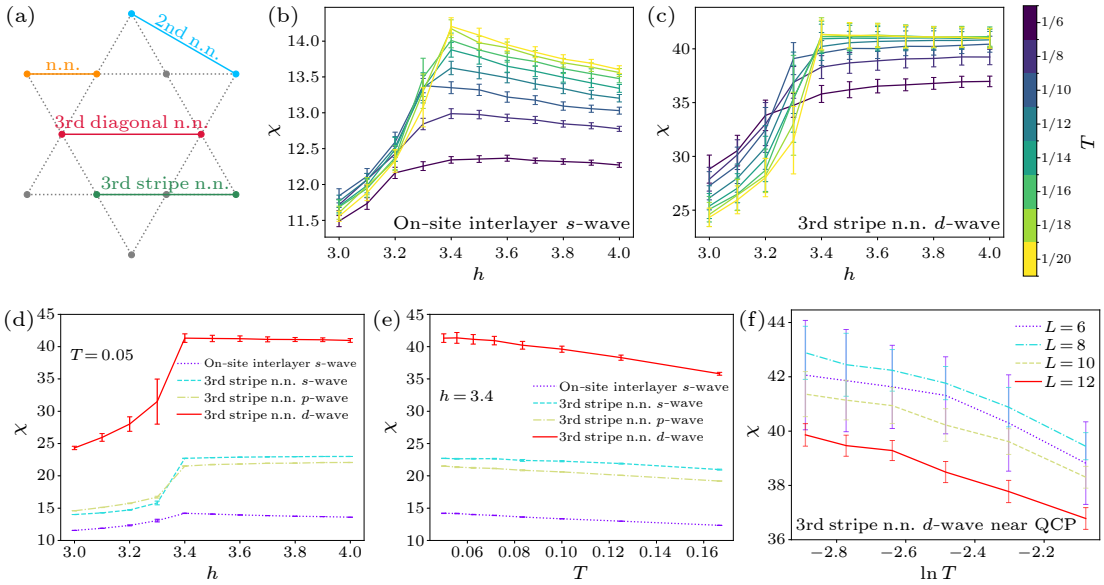

Fig. 4. Pairing susceptibilities of different channels. (a) Geometry of nearest-neighbor (n.n.), second n.n., and third n.n. pairings along the stripe and diagonal directions in the kagome lattice. (b) The s-wave pairing susceptibilities between two electrons on the same kagome site but in different layers. (c) Third stripe n.n. d-wave pairing. The color bar on the right represents temperature T in subfigures (b) and (c). (d) Comparison of different pairing channels at $L = 10$ and $T = 0.05$ as a function of h. (e) Comparison of different pairing channels at $L = 10$ and $h \approx h_c$ as temperature decreases. (f) Linear relationship between χ and $\ln T$ for third stripe n.n. d-wave superconductivity near the QCP, shown for all system sizes.

possibly due to its low transition temperature. We further show the susceptibilities of d-wave for different system sizes in Fig. 4(f) and they show logarithmic decrease with increasing T. However, susceptibility decreases when system size L increases from 8 to 10 and 12, suggesting that the finite-size effects is still significant. This is not surprising, given that the LCO is 2×2 and each unit cell contains three sites. Part of discrete Fourier transformation momenta $\boldsymbol{k}$ points for $L = 8$ perfectly lie on the Fermi surface with diverging density of state and huge contribution to pairing susceptibilities. Combining all these evidence, we can conclude that the system exhibits strong tendency towards d-wave superconductivity driven by the 2×2 loop-current fluctuations. The d-wave pairing is likely stemming from the repulsive Cooper pair scattering between VHSs mediated by the loop-current fluctuations. As previously mentioned, the sublattice texture associated with VHSs dictates a dominant intra-sublattice pairing. In the third n.n. channel, the pairing along stripe bonds is much stronger than along diagonal bonds because the former pairing can be mediated by the second order of local Ising spin fluctuations, whereas the latter requires at least third-order process. The two-fold d-wave pairing will form a $d + id$-wave pairing to gain condensation energy, which breaks the time-reversal symmetry and features a nontrivial Chern number. Therefore, the 2×2 loop-current fluctuations can drive a chiral d-wave pairing within the kagome lattice.

6. Discussion and Conclusion. Through model design and numerical calculation, we have revealed the many-body effects of 2×2 LCO on the electronic structure and loop-current fluctuation mediated d-wave pairing within the kagome lattice. Due to the significant finite-size effect with 2×2 order and kagome lattice, we do not observe a superconducting transition down to $T = 0.05$. However, our results provide clear evidence of d-wave pairing tendency from quantum fluctuations. In contrast to square lattice, the wave vectors with loop-current fluctuation are three-fold connecting three different VHSs. The interplay between loop-current fluctuation and sublattice texture on Fermi surface generates a two-fold intra-sublattice d-wave pairing, resulting a chiral d-wave state. These loop-current fluctuations may also generate non-Fermi liquid behaviors.

Our results have potential implications for kagome superconductors with LCO, such as AV_3Sb_5. In our model, the transverse field h can be linked to pressure or doping in experiments, which tunes the charge order. The enhanced superconductivity near the QCP of LCO is consistent with experimental observation of dramatic T_c enhancement when the CDW is suppressed with pressure or doping.[19] Moreover, the chiral d-wave pairing features a full gap and this aligns with nodeless gaps in recent ARPES measurements.[48] Loop-current fluctuations may induce a pairing density wave, which deserves future study.

In conclusion, we designed a sign problem-free bilayer kagome model coupled to Ising spin by the bond current, incorporating 2×2 loop-current fluctuations, and performed DQMC calculations to explore single-particle properties and superconductivity from loop-current fluctuations. We observe intriguing band folding, gap opening, and band broadening induced by LCO. Near the QCP of 2×2 LCO, the loop-current fluctuations enhance an intra-sublattice chiral d-wave pairing, owing to the unique sublattice texture associated with VHSs. To our knowledge, this is the first demonstration of loop-current fluctuation enhanced superconductivity within the kagome lat-

tice. Our results offer an alternative explanation for the T_c enhancement near QCP in kagome superconductors. Our work significantly deepens the understanding of LCO and impacts of the corresponding quantum fluctuations, thereby paving the way for elucidating underlying mechanisms of correlated states in quantum materials.

Acknowledgments. We thank Zi Yang Meng and Fakhar Assaad for valuable discussions. This work is supported by the National Natural Science Foundation of China (Grant No. 12447103). QFL acknowledges financial support from the MERIT-WINGS course provided by the University of Tokyo, and the Fellowship for Integrated Materials Science and Career Development provided by the Japan Science and Technology Agency. QFL further acknowledges support from the computational resource of Wisteria/BDEC-01 provided by Information Technology Center, the University of Tokyo, for the Monte Carlo simulation. WLJ acknowledges the support by the National Natural Science Foundation of China (Grant No. 12404275) and the Fundamental Research Program of Shanxi Province (Grant No. 202403021212015). GPP acknowledges support from the Würzburg-Dresden Cluster of Excellence on Complexity and Topology in Quantum Matter - ct.qmat (EXC 2147, Project No. 390858490). XYX is supported by the National Natural Science Foundation of China (Grant No. 12274289), the National Key R&D Program of China (Grant Nos. 2022YFA1402702 and 2021YFA1401400), the Innovation Program for Quantum Science and Technology (Grant No. 2021ZD0301902), Yangyang Development Fund, and Startup Funds from SJTU. XXW is supported by the National Key R&D Program of China (Grant No. 2023YFA1407300) and the National Natural Science Foundation of China (Grant No. 12047503).

References

[1] Ortiz B R, Gomes L C, Morey J R, Winiarski M, Bordelon M, Mangum J S, Oswald I W H, Rodriguez-Rivera J A, Neilson J R, Wilson S D, Ertekin E, McQueen T M, and Toberer E S 2019 *Phys. Rev. Mater.* **3** 094407

[2] Neupert T, Denner M M, Yin J X, Thomale R, and Hasan M Z 2022 *Nat. Phys.* **18** 137

[3] Jiang K, Wu T, Yin J X, Wang Z, Hasan M Z, Wilson S D, Chen X, and Hu J 2021 arXiv:2109.10809 [cond-mat.supr-con]

[4] Zhu H E, Li T R, Yu F H, Li Y L, Wang S, Wu Y B, Liu Z F, Shang Z M, Cui S T, Liu Y, Zhang G B, Zhang L D, Wang Z Y, Wu T, Ying J J, Chen X H, and Sun Z 2023 *Chin. Phys. Lett.* **40** 047301

[5] Wu L, Hu Y T, Fan D Z, Wang D, and Wan X G 2023 *Chin. Phys. Lett.* **40** 117103

[6] Yin J X, Jiang Y X, Teng X, Hossain M S, Mardanya S, Chang T R, Ye Z, Xu G, Denner M M, Neupert T, Lienhard B, Deng H B, Setty C, Si Q, Chang G, Guguchia Z, Gao B, Shumiya N, Zhang Q, Cochran T A, Multer D, Yi M, Dai P, and Hasan M Z 2022 *Phys. Rev. Lett.* **129** 166401

[7] Teng X, Chen L, Ye F, Rosenberg E, Liu Z, Yin J X, Jiang Y X, Oh J S, Hasan M Z, Neubauer K J, Gao B, Xie Y, Hashimoto M, Lu D, Jozwiak C, Bostwick A, Rotenberg E, Birgeneau R J, Chu J H, Yi M, and Dai P 2022 *Nature* **609** 490

[8] Teng X, Oh J S, Tan H, Chen L, Huang J, Gao B, Yin J X, Chu J H, Hashimoto M, Lu D, Jozwiak C, Bostwick A, Rotenberg E, Granroth G E, Yan B, Birgeneau R J, Dai P, and Yi M 2023 *Nat. Phys.* **19** 814

[9] Mielke C, Das D, Yin J X, Liu H, Gupta R, Jiang Y X, Medarde M, Wu X, Lei H C, Chang J, Dai P, Si Q, Miao H, Thomale R, Neupert T, Shi Y, Khasanov R, Hasan M Z, Luetkens H, and Guguchia Z 2022 *Nature* **602** 245

[10] Wu Q, Wang Z X, Liu Q M, Li R S, Xu S X, Yin Q W, Gong C S, Tu Z J, Lei H C, Dong T, and Wang N L 2021 arXiv:2110.11306 [cond-mat.supr-con]

[11] Guo C, Putzke C, Konyzheva S, Huang X, Gutierrez-Amigo M, Errea I, Chen D, Vergniory M G, Felser C, Fischer M H, Neupert T, and Moll P J W 2022 arXiv:2203.09593 [cond-mat.str-el]

[12] Xu Y, Ni Z, Liu Y, Ortiz B R, Wilson S D, Yan B, Balents L, and Wu L 2022 arXiv:2204.10116 [cond-mat.str-el]

[13] Guo C, Putzke C, Konyzheva S, Huang X, Gutierrez-Amigo M, Errea I, Chen D, Vergniory M G, Felser C, Fischer M H, Neupert T, and Moll P J W 2022 *Nature* **611** 461

[14] Ma H Y, Yin J X, Zahid Hasan M, and Liu J P 2024 *Chin. Phys. Lett.* **41** 047103

[15] Feng X, Jiang K, Wang Z, and Hu J 2021 *Sci. Bull.* **66** 1384

[16] Denner M M, Thomale R, and Neupert T 2021 *Phys. Rev. Lett.* **127** 217601

[17] Lin Y P and Nandkishore R M 2021 *Phys. Rev. B* **104** 045122

[18] Park T, Ye M, and Balents L 2021 *Phys. Rev. B* **104** 035142

[19] Chen K, Wang N, Yin Q, Gu Y, Jiang K, Tu Z, Gong C, Uwatoko Y, Sun J, Lei H *et al.* 2021 *Phys. Rev. Lett.* **126** 247001

[20] Varma C 1997 *Phys. Rev. B* **55** 14554

[21] Varma C 1999 *Phys. Rev. Lett.* **83** 3538

[22] Nakatsuji S, Kuga K, Machida Y, Tayama T, Sakakibara T, Karaki Y, Ishimoto H, Yonezawa S, Maeno Y, Pearson E, Lonzarich G G, Balicas L, Lee H, and Fisk Z 2008 *Nature Physics* **4** 603

[23] Matsubayashi K, Tanaka T, Sakai A, Nakatsuji S, Kubo Y, and Uwatoko Y 2012 *Phys. Rev. Lett.* **109** 187004

[24] Sakai A, Matsumoto Y, Fu M, Isomae T, Tsujimoto M, O'Farrell E, Nishio-Hamane D, and Nakatsuji S 2025 *Nat. Commun.* **16** 2114

[25] Palle G, Ojajärvi R, Fernandes R M, and Schmalian J 2024 *Sci. Adv.* **10** eadn3662

[26] Cai G H, Jiang Y T, Zhou H, Yu Z, Jiang K, Shi Y G, Meng S, and Liu M 2023 *Chin. Phys. Lett.* **40** 117101

[27] Yu S L and Li J X 2012 *Phys. Rev. B* **85** 144402

[28] Kiesel M L and Thomale R 2012 *Phys. Rev. B* **86** 121105

[29] Wang W S, Li Z Z, Xiang Y Y, and Wang Q H 2013 *Phys. Rev. B* **87** 115135

[30] Kiesel M L, Platt C, and Thomale R 2013 *Phys. Rev. Lett.* **110** 126405

[31] Wu X, Schwemmer T, Müller T, Consiglio A, Sangiovanni G, Di Sante D, Iqbal Y, Hanke W, Schnyder A P, Denner M M, Fischer M H, Neupert T, and Thomale R 2021 *Phys. Rev. Lett.* **127** 177001

[32] Fu R Q, Zhan J, Dürrnagel M, Hohmann H, Thomale R, Hu J, Wang Z, Zhou S, and Wu X 2024 arXiv:2405.09451 [cond-mat.str-el]

[33] Blankenbecler R, Scalapino D J, and Sugar R L 1981 *Phys. Rev. D* **24** 2278

[34] Scalapino D J and Sugar R L 1981 *Phys. Rev. B* **24** 4295

[35] Assaad F and Evertz H 2008 *Computational Many-Particle Physics* (Springer Berlin Heidelberg, Berlin, Heidelberg) p. 277

[36] Wu C and Zhang S C 2005 *Phys. Rev. B* **71** 155115

[37] Assaad F F, Bercx M, Goth F, Götz A, Hofmann J S, Huffman E, Liu Z, Toldin F P, Portela J S E, and Schwab J 2022 *SciPost Phys. Codebases* 1
[38] Blöte H W J and Deng Y 2002 *Phys. Rev. E* **66** 066110
[39] Mayo S G, Yndurain F, and Soler J M 2020 *J. Phys.: Condens. Matter* **32** 205902
[40] Sandvik A W 1998 *Phys. Rev. B* **57** 10287
[41] Beach K S D 2004 arXiv:cond-mat/0403055 [cond-mat.str-el]
[42] Sandvik A W 2016 *Phys. Rev. E* **94** 063308
[43] Shao H, Qin Y Q, Capponi S, Chesi S, Meng Z Y, and Sandvik A W 2017 *Phys. Rev. X* **7** 041072
[44] Wu X, Schwemmer T, Müller T, Consiglio A, Sangiovanni G, Di Sante D, Iqbal Y, Hanke W, Schnyder A P, Denner M M, Fischer M H, Neupert T, and Thomale R 2021 *Phys. Rev. Lett.* **127** 177001
[45] Abrikosov A A, Dzyaloshinskii I, Gorkov L P, and Silverman R A 1975 *Methods of quantum field theory in statistical physics* (Dover, New York)
[46] Jiang W, Liu Y, Klein A, Wang Y, Sun K, Chubukov A V, and Meng Z Y 2022 *Nat. Commun.* **13** 2655
[47] Schattner Y, Gerlach M H, Trebst S, and Berg E 2016 *Phys. Rev. Lett.* **117** 097002
[48] Zhong Y, Liu J, Wu X, Guguchia Z, Yin J X, Mine A, Li Y, Najafzadeh S, Das D, Mielke III C *et al.* 2023 *Nature* **617** 488